Available online at www.sciencedirect.com

ScienceDirect

Procedia Computer Science 1 (2012) 673–680

Procedia Computer Science

www.elsevier.com/locate/procedia

International Conference on Computational Science, ICCS 2010

VOF Simulation of Marangoni Flow of Gas Bubbles in 2D-axisymmetric Column

Y. Alhendal[a]*, A. Turan[a], Wael I. A. Aly[b]

[a]*School of Mechanical, Aerospace and Civil Engineering, University of Manchester, UK*

[b]*Department of Refrigeration and Air Conditioning Technology, Faculty of Industrial Education, Helwan University, 11282 Cairo, Egypt*

Abstract

The migration of gas bubbles immersed in a liquid under the action of temperature gradient and surface tension (Marangoni flow) in zero gravity environment is numerically investigated for different Ma, Re, and Pr (Marangoni, Reynolds, and Prandtl numbers). The full Navier–Stokes equations as well as the energy equation for temperature gradient are solved by a volume of fluid (VOF) method/Finite Volume method, and the surface tension force is modeled by a continuum surface force (CSF) model. The behavior of bubble migrating toward the hotter side by the action of surface tension using the flow relations between two bubbles (leading and trailing bubble), and the trajectories and the velocities of the different bubbles diameters, in microgravity environment have been investigated numerically. It has been verified that the calculated results are in good agreement with available experimental and numerical results. It is also concluded that the VOF is able to simulate two-phase flow under zero gravity conditions.

Keywords: Marangoni Flow; Zerogravity; Bubbles; VOF

1. Introduction

Marangoni bubbly flow, which is the migration of bubbles due to surface tension gradients, is the main subject of this paper. The investigation of how the process parameters affect the bubble migration has become an attractive area for researchers recently. This investigation has very important applications for recent and future live in microgravity areas, such as chemical, industrial and petroleum engineering applications. On the other hand, structure academic study needs to investigate this phenomenon in details and conclude different parameters for different study application such as kernels function which can be used in population balance equations. Marangoni flow could be a gravity replacement for fluid flow simulation in microgravity application. In 1959, Young et al. [1] first investigated the thermocapillary migration of bubbles and drops with their linear model, which is suitable for small Reynolds number (Re) and small Marangoni number (Ma). Few low-gravity experiments have been carried out up to date, and the most extensive data were presented by Thompson and DeWitt [2], who used the drop tower at NASA Lewis

* Corresponding author. Tel.: +044-161-275-4368; fax: +044-161-306-3729.
E-mail address: yousuf.alhendal@postgrad.manchester.ac.uk.

1877-0509
doi:10.1016/j.procs.2010.04.072

Balasubramaniam and Lavery [4] have also been obtained by Treuneret et. al. [5] who showed results of drop tower experiments concerning thermocapillary bubble migration at high Reynolds and Marangoni numbers and noted complicated transients and time-dependent behaviour in regimes where the flow has finite viscous and thermal inertia. They also show a good comparison with [2]. Recently, Kang et. al. [6] reached the maximum Ma of bubble thermocapillary migrations of 9288, which is larger than any previous space experiments. Their results of the bubbles migration velocity confirmed the trend predicted by Balasubramaniam and Subramanian [7].
Investigations of the Marangoni motion of bubbles can only conducted in a low-gravity environment such as sounding rockets, drop towers, and aboard space shuttles. Some previous experiments have noted complex transients and time-dependent behaviour in regimes where the flow has finite viscous and thermal inertia and noted the needed for theoretical and numerical results with which to compare their experimental results and to improve the physical understanding, and to support the interpretation of experimental results [5]. In the present study a numerical method of finite-volume/VOF model has been verified and validated using both theoretical and experimental data to compute the Marangoni forces of single and multi bubbles migration. It is also show the main factors around rising single and multi bubbles which help understanding the actual mechanisms of bubble behaviour in reduced gravity and their coalescence mechanism.

The parameters characterizing Marangoni bubble migration, as revealed by the steady-state momentum and energy equations, are the Reynolds and the Marangoni numbers which are coupled by the Prandtl number

$$\mathrm{Re} = \frac{RU}{\nu} \tag{1}$$

$$Ma = \frac{RU}{\alpha} \tag{2}$$

$$\mathrm{Pr} = \frac{\nu}{\alpha} \tag{3}$$

$$\alpha = \frac{k}{\rho\, Cp} \tag{4}$$

where R is the radius of the bubble; U is the measured local migration velocity, ν is the kinematic viscosity, α is the thermal diffusivity; k and Cp are the thermal conductivity and the specific heat of the continuous phase; ρ is the density of the continuous phase. No turbulence model was used in this simulation, using a turbulence model gives unphysical results for both VOF and Euler-Euler models [3]. All simulation were run at time t = 0 with initial stationary liquid and gas with applicable surface tension between ethanol and nitrogen σ = 27.5 (dyn/cm), and surface tension gradient $d\sigma/dt$ (σt) = -0.09 (dyn/cm ºC), Kuhlmann [8]. σ is the coefficient of surface tension:

$$\sigma = \sigma_0 + \sigma_T (T_0 - T) \tag{5}$$

where σ_0 is the surface tension at a reference temperature T_0, and σ_T is a constant depending on the fluid type used in the simulation.

2. Governing Equations, Numerical Scheme, and Boundary Conditions

2.1. Modeling Equations (VOF)

The volume fraction equation for the q-th phase:

$$\frac{\partial \alpha_q}{\partial t} + \bar{v}\nabla \alpha_q = \frac{S_{\alpha_q}}{\rho_q} \tag{6}$$

In the VOF model, the geometric reconstruction scheme that is based on the piece linear interface calculation (PLIC) method is applied to reconstruct the bubble-free surface. It assumes that the interface between two fluids has a linear slope within each cell, and uses this linear shape for calculation of the advection of fluid through the cell faces. The first step in this reconstruction scheme is calculating the position of the linear interface relative to the centre of each partially filled cell, based on information about the volume fraction and its derivatives in the cell. The second step is calculating the adverting amount of fluid through each face using the computed linear interface representation and information about the normal and tangential velocity distribution on the face. The third step is to calculate the volume fraction in each cell using the balance of fluxes calculated during the previous step, Akhtar [9].

A single momentum equation is solved throughout the domain, and the resulting velocity field is shared among the phases:

$$\frac{\partial}{\partial t}(\rho\vec{v}) + \nabla(\rho\vec{v}\vec{v}) = -\nabla p + \nabla.[\mu(\nabla\vec{v} + \nabla\vec{v}^T] + \rho g + \vec{F} \tag{7}$$

The density ρ and dynamic viscosity μ in the equation are dependent on the volume fraction of all phases:

$$\rho = \sum \alpha_q \rho_q \tag{8}$$

$$\mu = \sum \alpha_q \mu_q \tag{9}$$

The energy equation is also shared among the phases:

$$\frac{\partial}{\partial t}(\rho E) + \nabla.[\vec{v}(\rho E) + p)] = \nabla.(\kappa_{eff}\nabla T) + S_h \tag{10}$$

The VOF model treats energy, E, and temperature, T, as mass-averaged variables:

$$E = \frac{\sum_{q=1}^{n} \alpha_q \rho_q E_q}{\sum_{q=1}^{n} \alpha_q \rho_q} \tag{11}$$

where E_q for each phase is based on the specific heat of that phase and the shared temperature. The effective thermal conductivity k_{eff} is also shared by the phases. The source term, S_h, contains contributions from radiation, as well as any other volumetric heat sources.

2.2. Boundary Conditions

For the model numerical domain shown in Fig. 1, the following assumptions are made in the analysis:

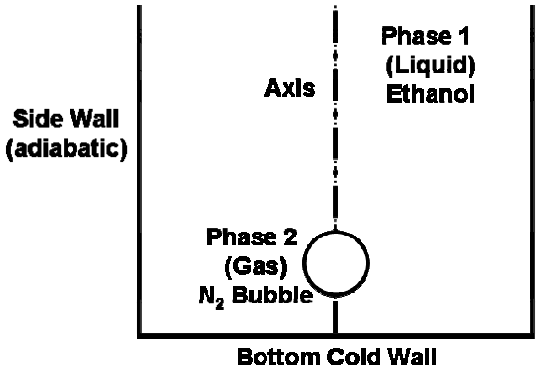

Fig. 1. Numerical Domain

1. Motion is 2D axisymmetric in cylindrical coordinates
2. Heat flux is zero at the bubble interface
3. Incompressibility of the liquid
4. Constant physical properties except for surface tension (UDF has been used)
5. Gravitational acceleration is zero

The vertical line denoted 'axis' signifies the axis of symmetry. Two horizontal walls (top and bottom) are separated by a distance H equal to 12 cm. The upper horizontal wall is no slip with constant temperature T_h= 330K, the lower horizontal wall is also no slip with constant temperature T_c = 300K. The domain was defined as a cavity with abounded walls. For all simulations the initial state will be set with no velocity at the inlet, nor at the outlet, and the pressure will be taken equal to the atmospheric pressure. The unsteady two dimensional 2D axisymmetric model of the problem was formulated using the commercial software package FLUENT® version 6.3. for modelling the climb of a bubble in a column of liquid in zero gravity (Marangoni flow).

3. Numerical Procedure

3.1. Using Fluent, Grid independence, and experimental case validation

Concerning the number of cells, We have found that a good compromise between the time for one iteration and a sufficient number of cells in the bubble was to use a grid made of an estimated 90000 cells, that is to say for axis 600 x 150. Another important point is that, when using the axisymmetric solver, we create a mesh only for the half of the domain, thus reducing drastically the number of cells used, and consequently the time of calculation. FLUENT® will accept the axis in the direction of the positive X-axis only.

Grid independence was achieved by increasing the number of structurally arranged quadrilateral cells from 45,000 (450 x 100) to 90,000 (600x150) and plotting the convergence of certain parameters of interest such as bubble migration time, bubbles coalescence time and distance, contours of temperature and stream lines. To validate the numerical procedure, results were compared with experimental data provided by Tomphson et al. [2] and Treuneret et. al. [5], and were found to be acceptable as shown in Fig. 2. The validation was done with an existing experimental data [2], through simulation of 0.5 cm N_2 bubble placed 1-cm from the bottom wall (cold). Hence the size of the axissymmetric computational wall bounded domain Fig. 1. was chosen as 12 cm x 6 cm with no "inflow or overflow" from the sides. For the purposes of these simulations, Ethanol properties were taken to be same as those given in reference [2]. Surface tension and its coefficient used in the simulations for the Ethanol are (σ = 27.5 dynes/cm and σ_T = -0.09 dynes/cm.°C) [8]. Material properties should be defined for each phase. The Boussinesq

et al.[2]. PISO scheme is used for Pressure-Velocity Coupling and PRESTO scheme used for pressure discretization. All other options (including under-relaxation factors) will be kept as default. The volume-of-fluid (VOF) approach implemented in FLUENT® has been used for axissymmetry simulations. The effect of Prandtl (Pr) number was considered. Figures 3 and 4 show the present simulation for two different liquids, Ethanol (Pr =16.3) and Methanol (Pr =6.88), and Nitrogen bubbles have been used. The figures present the volume fraction, temperatures contours, and stream lines after 4.6 seconds. The bubble displacement of 5 cm after 4.6 seconds (Fig. 3) is very close to the experimental results of Tomphson et al.[2], their experimental zero-gravity measurements for a nitrogen bubble in

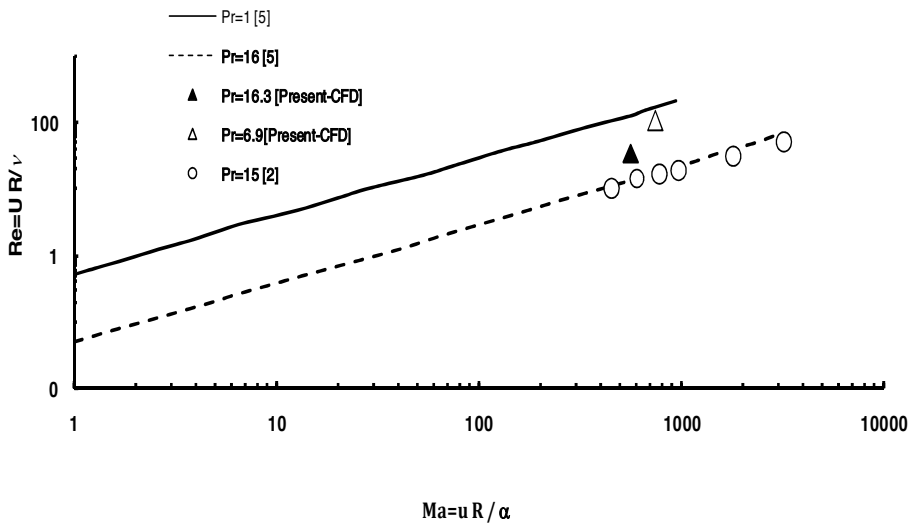

Fig. 2. The relation between Reynolds number and Marangoni number at different Prandtl numbers.

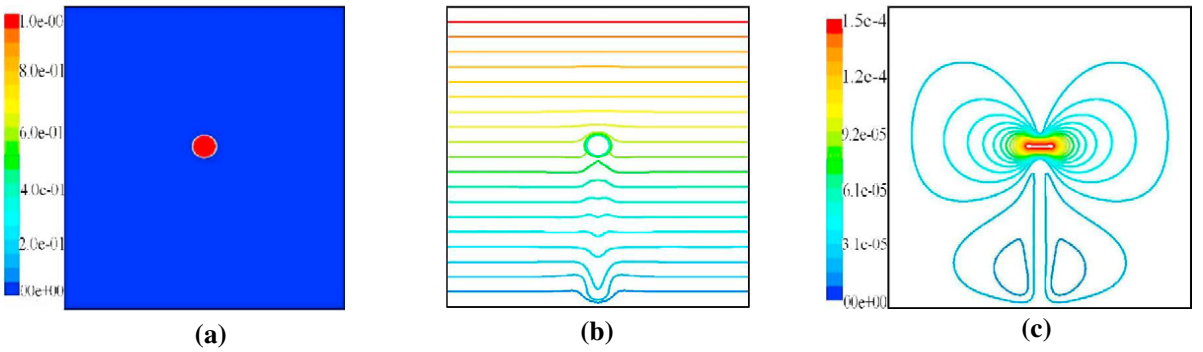

Fig.3. (a) Volume fraction (b) Temperature, and (c) Stream lines for Pr =16.28 (Ethanol) at t=4.6 at a distance of 5 cm

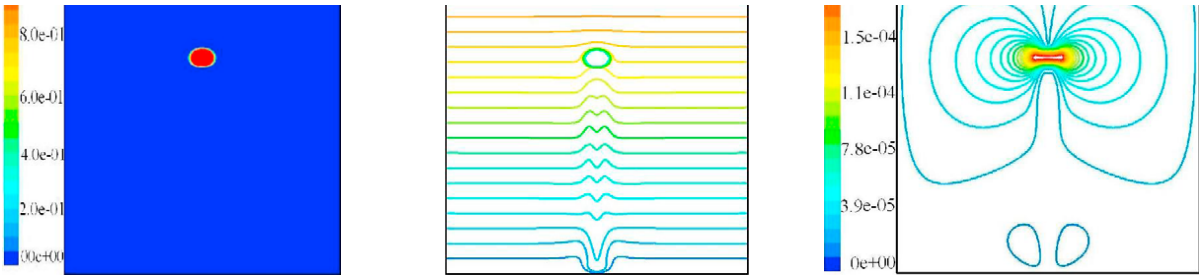

Fig.4. (a) Volume fraction (b) Temperature, and (c) Stream lines for Pr =6.88 (Methanol) at t=4.6 at a distance of 7 cm

ethanol subjected to a linear temperature gradient were obtained using the NASA Lewis zero-gravity drop tower. The effect of Prandtl number is seen in both figures, decreasing Pr increases the bubble displacement. The bubble rise velocity, and shape has also been compared with the experimental data available in the literature and a good agreement was obtained between experiments and CFD-Fluent simulation. The present trends of the bubble migration stream line and temperature contours (Figs. 3 and 4, b-c) are in good agreement with the work of Nas and Tryggvason's [10].

4. Results and Discussion

The interaction of two bubbles (a small bubble with radius of 0.25 cm and a big bubble with radius of 0.5 cm) is investigated in three different cases, namely:

1- Small bubble on top of big bubble.
2- Big bubble on top of small bubble.
3- Two equal radius bubbles.

Figure 5. shows the initial placement of the bubbles in the three cases for the computations presented in this section.

Case [1]

Two gas bubbles, big (R_{big}= 0.5 cm) and small (R_{small}= 0.25 cm), are initially located at (1.5, 0.0) and (3.25, 0.0), respectively, in the domain of a size (6x12 cm). The simulation results showed that the big bubble moves faster than the small bubble, the velocity of the big bubble about twice that of the small bubble as shown in Fig. 6. The big bubble approaches the small bubble within 2.257 s, and the two bubbles then eventually merged.

Case [2]

Two gas bubbles, big (R_{big}= 0.5 cm) and small (R_{small}= 0.25 cm), are initially located at (3.25 cm, 0.0) and (1.5 cm, 0.0), respectively, in the domain of a size (6x12 cm). The simulation results showed that the big bubble moves faster than the small bubble, the velocity of the big bubble about triple that of the small bubble as shown in Fig. 7. The small bubble did not approach the big bubble, and the two bubbles did not merge.

Case [3]

Two gas bubbles of equal radius, (R= 0.5 cm), are initially located at (1.5cm, 0.0) and (3.25, 0.0), respectively, in the domain of a size (6x12 cm). The simulation results showed that the two bubbles move together with almost same velocity, then the upper bubbles moves a little faster when approaching the top hot wall (Fig. 7). The two bubbles did not merge.

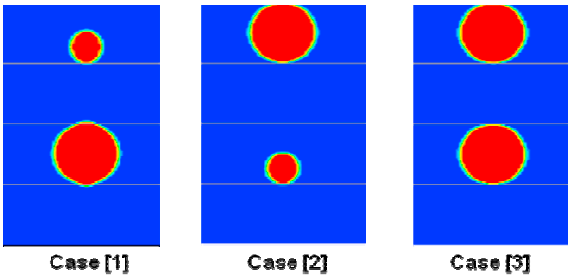

Fig. 5. The initial conditions for the three cases.

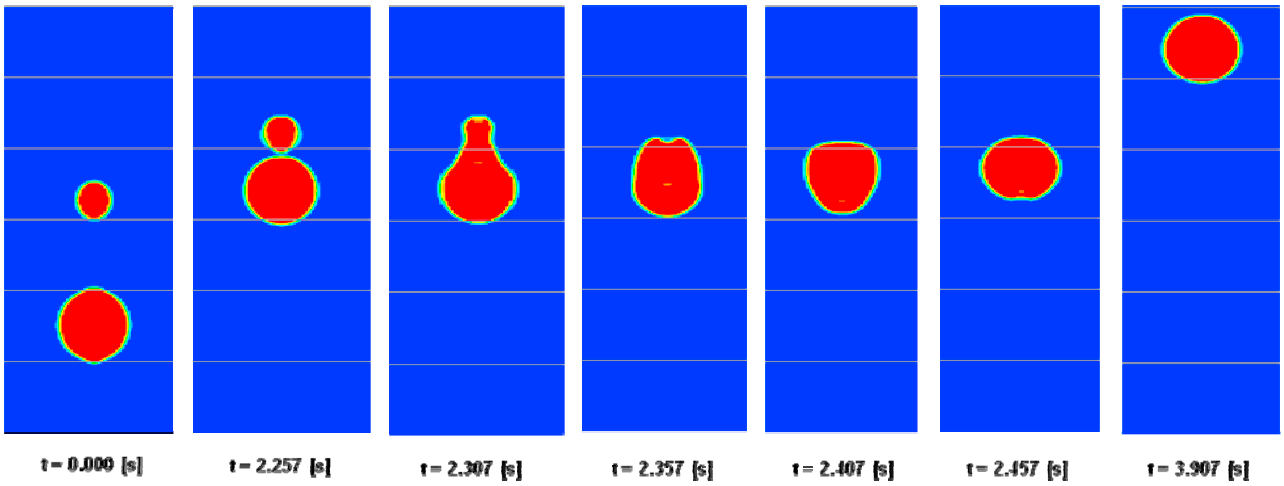

Fig. 6. Coalescence process at the time intervals for case 1.

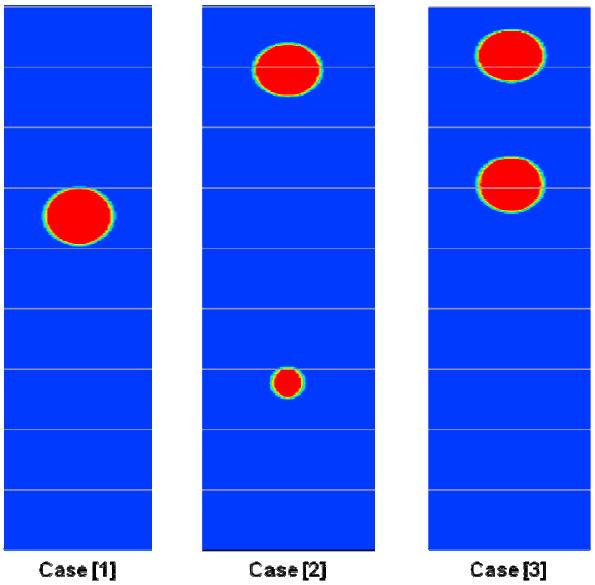

Fig. 7. The three cases after 4 seconds from the start of simulation.

interface leads to shear stresses that act on the outer fluid by viscous forces, thus inducing a motion of the fluid bubble in the direction of the thermal gradient as shown from Fig. 7. Temperature gradients cause surface tension gradients at the liquid-gas interface (meniscus), and the variation of surface or interfacial tension along the meniscus gives rise to convection. The flow from a region of low surface tension to a region of higher surface tension is referred to as Marangoni flow, this phenomena is more clear in Figures 3 and 4. The motion of the bubble creates a motion of the liquid around it. This motion of the ethanol reflects at the bottom of our domain and then comes back in the back of the bubble.

5. Conclusions

In this paper, we have numerically investigated the thermocapillary migration (Marangoni effect) of spherical bubbles in continuous phase fluid under the variation of temperature gradient. VOF model is used in the present study to solve this transition case. It is concluded that VOF is a robust numerical method for the simulation of gas-liquid two-phase flows with high density ratios under zero gravity conditions. The coalescence process of two gas bubbles under different cases are revealed and compared in this paper.

In the future, this work will be extended to three dimensional cases (3D) and a rotational effect will be considered. Also, more detailed discussions for different breakage and coalescence times for a group of bubbles will be investigated and used to make kernels function which can be used in population balance equations.

References

1. Young, N.O., Goldstein, J.S., Block, M.J., The motion of bubbles in a vertical temperature gradient, J. Fluid Mech. 6 (1959) 350-356.
2. Thompson, R.L., DeWITT, K.J. and Labus, T.L., Marangoni Bubble Motion Phenomenon in Zero Gravity, Chemical Engineering Communications 5 (1980) 299-314.
3. Chen L. and Manasseh R., Proc. 4th Int. Conf. on Multiphase Flow, New Orleans, LA, USA, 27 May to 1 June 2001, ed. E.E. Michaelides (2001) paper no. 348.
4. Balasubramaniam, R., Lavery, J.E., Numerical Simulation Of Thermocapillary Bubble Migration Under Microgravity for Large Reynolds and Marangoni Numbers, Num. Heat Transfer A 16 (1989) 175-187.
5. Treuner, M., Galindo, V., Gerbeth, G., Langbein, D., Rath, H. J., Thermocapillary Bubble Migration at High Reynolds and Marangoni Numbers Under Low Gravity. J. Colloid Interface Sci. 179 (1996) 114-127.
6. Kang Q., Cui H. L., Hu L., Duan L., On-board Experimental Study of Bubble Thermocapillary Migration in a Recoverable Satellite, Microgravity Sci. Thermal 20 (2008) 67-71.
7. Balasubramaniam, R. and Subramanian, R.S., Thermocapillary Bubble Migration-Thermal Boundary Layers For Large Marangoni Numbers, Int. J. Multiph. Flow 22(1996) 593-612.
8. H.C. Kuhlmann, Thermocapillary Convection in Models of Crystal Growth, 152**,** Springer, Berlin, Heidelberg (1999) Springer Tracts in Modern Physics.
9. Akhtar, A., V. Pareek and M. Tade, 2007. CFD simulations for continuous flow of bubbles through gas-liquid columns: Application of VOF method. Chem. Prod. Process Model., 2: 1-19.
10. Nas S. and Tryggvason G., Computational Investigation of the Thermal Migration of Bubbles and Drops, AMD 174/FED 175 Fluid Mechanics Phenomena in Microgravity, Ed. Siginer, Thompson, and Trefethen. ASME Winter Annual Meeting, (1993) 71-83.